

Structure of VLF Whistler Mode Sideband Waves in the Magnetosphere

L. A. D. SÁ AND R. A. HELLIWELL

Space, Telecommunications and Radioscience Laboratory, Stanford University, Stanford, California

An accurate determination is made of the sideband structure of ducted VLF whistler mode waves transmitted from Siple Station and observed at Lake Mistissini, Quebec. Single- and double-frequency experiments are described. It is shown that sideband spectra can be explained by nonlinear interactions between two or more lines in the magnetosphere, the line intensities required for such interactions being low. If one of the lines is a transmitted carrier, the other line can be as much as 40 dB lower in amplitude, implying that power line radiation (PLR) can be an important factor in sideband generation. It is shown that "single-line" sidebands are due to interactions between the input wave and harmonics of 60 Hz present within the duct (assumed to be PLR), and that double-line spectra are affected by their position relative to the same 60-Hz system of lines. A study of double-line spectra as a function of line separation and line amplitude ratio is made.

1. INTRODUCTION

Whistler mode sidebands generated by the Siple Station transmitter have been the subject of several papers, some of them mainly descriptive, such as Park [1981], others, such as Helliwell *et al.* [1986], also presenting a mechanism for the observed sidebands. A shortcoming noted in those papers was the lack of a unifying idea that could shed some light on the cause and structure of all observed spectra, indicating relevant variables and suggesting experiments in which the mechanism of spectra formation could be investigated. As a result of such a lack, only for the case of double carrier transmission [Helliwell *et al.*, 1986], where the sideband spectra consist mainly of harmonics of the carrier frequency separation, was it possible to arrive at a successful description of the line structure together with a possible mechanism for its creation.

In this paper, such a unifying idea is put forward, together with a set of experimental data showing its plausibility. In a forthcoming theoretical paper the same idea will be justified from a mathematical viewpoint, and many of its consequences will be further explored.

2. SIDEBAND GENERATION MECHANISM

The basic assumption used to analyze the data in this paper is a property common to many nonlinear dynamical systems, being mentioned and discussed, for instance, by Chirikov [1979]. In the present paper, we quote this property without proof and justify it simply by the accurate way in which it describes the data. It may be stated as follows:

If several lines with frequencies $\Omega_i, i = 1 \dots n$, measured from one of the carriers, are present in the magnetosphere, they are able to interact with one another, and a new line can be created at a frequency Ω , given by

$$m\Omega = m_1\Omega_1 + \dots + m_n\Omega_n \quad (1)$$

where m and m_i are arbitrary integers ($m \neq 0$). The likelihood of a line being created depends partly on the underlying

electron distribution and incoming line intensities, but is higher the smaller the integers in question are and the smaller the number of lines involved in the interaction is.

As an example we can look at the two-line case: If only two lines are initially present, one of the frequencies will be zero, and the other will be the frequency separation between the lines, $\Delta\Omega$. Then

$$q\Omega = p\Delta\Omega \quad (2)$$

This means that a line can be created at any rational point between the original two lines, small values for p and q being more likely to occur. Equation (2) predicts the occurrence of harmonics ($q = 1$, any p), half harmonics ($q = 2, p = 1$), one-third harmonics ($q = 3, p = 1, 2$), etc.

For three lines, with subscripts 1, 2, 3, an interesting result is obtained for a particular choice of the smallest nonzero values of the integer coefficients:

$$\Omega = \Omega_2 - \Omega_3 \quad (3)$$

For $\Omega_2 \geq \Omega_3$ this implies the creation of a mirror image of line 3, within the interval defined by lines 1 and 2, as shown in Figure 1.

Other sign combinations in (3) are possible, but lead to rarely found lines. For instance, a plus instead of a minus sign in (3) will describe an intermodulation effect:

$$\Omega = \Omega_2 + \Omega_3 \quad (4)$$

Although infrequently seen, an example of this effect is found in Figure 4h, and is described in section 4.

3. DESCRIPTION OF EXPERIMENTAL METHODS

Most of the data discussed in this paper came from the CISP (carrier interaction with simulated power line) program, transmitted from Siple Station and received at Lake Mistissini, Quebec, after ducted whistler mode propagation. Its format consists of a sequence of 3-s pulses, 10 s apart, each one made up of a pair of single-frequency carriers with defined amplitude ratio and frequency separation, as shown in Figure 2. The position of the upper carrier is fixed at a power line harmonic frequency, its amplitude being a variable parameter. The amplitude of the lower carrier is kept constant, but its position below the upper carrier can be varied. The transmitted upper to lower carrier amplitude

Copyright 1988 by the American Geophysical Union.

Paper number 7A9341.
0148-0227/88/007A-9341\$02.00

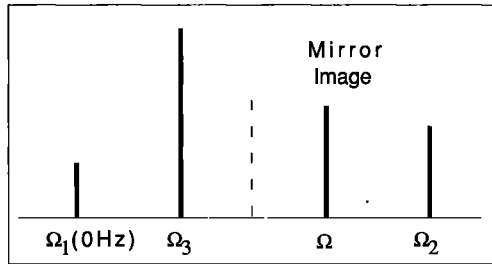


Fig. 1. Mirror image sideband creation. Dashed line marks symmetry axis.

ratio can be set to -20 dB, -30 dB, -40 dB, or minus infinity. The carrier frequency separation can be 20 Hz, 23 Hz, 30 Hz, 37 Hz, 40 Hz, and 60 Hz.

Those frequency and amplitude ratio values are chosen with power line radiation (PLR) effects in mind. The reason for choosing such amplitude ratios is that PLR levels in the magnetosphere are believed to be 30 dB or more below the carrier amplitude levels. Since signals with such low amplitudes are not directly detectable, a possible PLR presence, together with its effects, must be verified by studying the effects produced on the spectra by weak lines radiated by the transmitter together with the main carrier.

The frequency separations consist of two groups: The first group, 20 Hz, 30 Hz, 40 Hz, 60 Hz, consisting of submultiples of 60 Hz, is chosen such that the carrier frequency separation is a rational function of the PLR line separation. This allows for the establishment of a resonance condition between the transmitted radiation and the one present in the duct. Under those circumstances, both systems can excite essentially the same lines, creating an easily understood spectrum. The second group, 23 Hz, 37 Hz, is chosen such that the carrier frequency separation is either the most irrational function of 60 Hz possible, the golden mean of 60 Hz [see Berry, 1978], or its complement with respect to 60 Hz. This choice does not allow easy excitation of the rational modes described above, resulting in the appearance of more complex line interactions such as the one responsible for the creation of mirror image sidebands.

4. DESCRIPTION OF DATA

Figure 3 shows a sequence of transmissions made with a constant line separation of 30 Hz, a very rational function of 60 Hz, and amplitude ratio varying from -20 dB to minus infinity. It can be seen that, as the upper carrier becomes weaker, the two carrier spectra blend in smoothly with the single carrier spectrum shown at the bottom right. For this particular set of transmissions it can also be seen that the line intensities in each pulse exhibit two maxima. Although the reason for the existence of such maxima will not be discussed in this paper, their presence provides a way of testing the reproducibility of the sideband structures, as described below.

Figure 4 displays the same sequence of pulses in a way that allows for easy and accurate measurements of frequency separations and relative line amplitudes. Each picture shows a 0.5s (or more) average of the spectrum. In each row, the first plot (A scan) comes from an average over the first, and the second plot over the second maximum in the pulse.

The averages are taken over the time intervals marked by solid horizontal bars at the bottom of each picture shown in Figure 3. Comparison of two A scans in the same row shows how reproducible the spectra are. The vertical lines in each plot locate multiples of 60 Hz where low-intensity PLR may be present. Figures 4a and 4b show the 20 dB ratio spectrum. The structure is almost what should ideally be expected. The two carriers create harmonics, which in turn create several half harmonics between them. Frequency distortion is minimal, all lines being at their theoretical positions within one filter bandwidth (1.56 Hz). Figures 4c and 4d show the 30 dB spectrum. Because of enhanced growth at the upper carrier, frequency distortion increases both for harmonics and sub harmonics. The bandwidth of each spectrum is also slightly decreased. Figures 4e and 4f show the 40 dB spectrum. The upper carrier would not be seen in this plot without the help of large temporal and differential growth with respect to the lower carrier (32 dB average). The lower carrier also goes through a pronounced growth process, adding to frequency distortion effects. Since growth is a function of the instantaneous electron distribution, reproducibility of the spectrum decreases (Figures 4e and 4f are fairly different). Increased initial amplitude asymmetry between the carriers encourages the appearance of sub harmonics different from the simple half harmonic. The harmonics initially seen in the 20 dB and 30 dB transmissions have now all but disappeared, more closely spaced harmonics being seen instead.

A detailed analysis of Figure 4e reveals the following line configuration: Line 2 is a harmonic of 5 and 7. Line 4 is a harmonic of 5 and 6. Line 3 is a half harmonic of 2 and 4. Line 9 is a one-third harmonic of 7, the upper carrier, and 10, a PL harmonic. Line 8 is a half harmonic of 7 and 9. Line 6 is simultaneously a one-fourth harmonic of 1 and 7, and a one-third harmonic of 5 and 7.

Lines such as line 9 are strongly excited because the sequence of sidebands behaves in this case as an incipient triggered emission. Energy is transferred upward from the carrier, is reflected at line 9, lingers around line 8, and is partly returned to the lower carrier, as shown in Figure 3.

Figure 4f has approximately the same structure as Figure 4e with some lines missing. Line 6 in Figure 4f is a half harmonic of 4 and 7.

Figures 4g and 4h show the single carrier spectrum. All sidebands now are coming from interactions between the

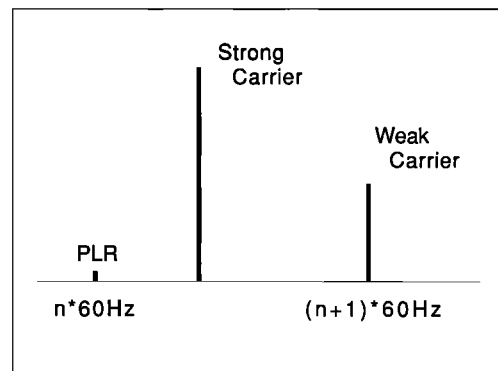


Fig. 2. CISF format used in sideband structure analysis described in this paper.

LM 08 JAN 87

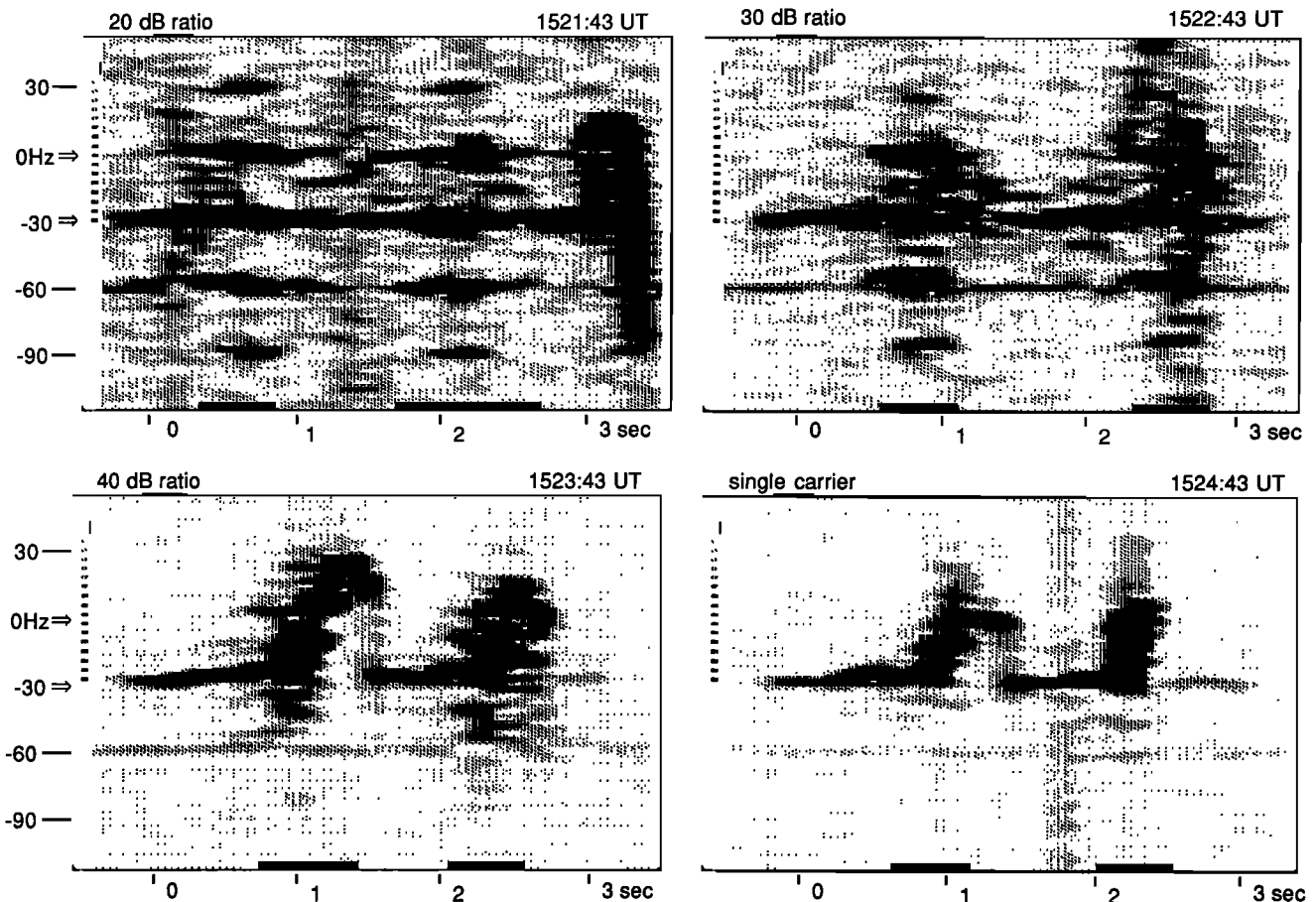


Fig. 3. Sequence of 3-s pulses with carrier separation equal to 30 Hz. 0 Hz in those pictures corresponds to 2220 Hz. The arrows point to the location of the two carriers. The horizontal bars at the bottom of each picture indicate the time intervals over which the average spectra shown in Figure 4 were taken. In all spectra the filter bandwidth was 1.56 Hz.

carrier and the residual PLR present in the duct. Since PLR forms a system of harmonic lines, we should expect the presence of multiple lines to influence the spectra.

In Figure 4g, line 4 is a half harmonic of 3 and the adjacent PL harmonic (not numbered in the picture). Line 7 is a one-third harmonic of the same PL with line 8 which also is a PL harmonic. Line 5 is simultaneously a half harmonic of 3 and 7, and a one-fourth harmonic of 3 and 8. Line 6 is a half harmonic of 5 and 7. Line 2 is simultaneously a harmonic of 4 and 6, and a one-third harmonic of the two PL harmonics immediately above and below it.

In Figure 4h, lines 4 and 5 are one-third harmonics of 3 and 7. Lines 2 and 8 are harmonics of 3 and 5. Line 6 is simultaneously a half harmonic of 5 and 7, and a one-fourth harmonic of 3 and the next PL harmonic above 7. Line 1 is a case of intermodulation: line 6 interacting with two PLs (theory requires them to be line 7 and the PL immediately above it), creates a line below itself at a distance of 60 Hz, the PLs' frequency separation.

Figure 5 shows a sequence of pulses with carrier separation kept at 37 Hz, the most irrational possible function of 60 Hz, with amplitude ratios varying from -20 dB to minus infinity. Figure 6 shows the corresponding sequence of A scans from which average frequencies and amplitudes are measured. Due to the irrationality of the frequency ratios in-

volved, few rational sub harmonics are excited, allowing for the creation of a particularly simple and repeatable spectrum. For each pulse there is now a single average made over the region where sidebands are present.

Figure 6a shows the basic structure which is approximately repeated in Figures 6b and 6c. Line 1 is simply a harmonic of 4 and 7. Line 5 is special: it is the mirror image of 4 in the interval defined by 2 and 7 (it is therefore a three-line effect involving two carriers and one PL harmonic). Line 3 is a harmonic of 4 and 5. Line 6 is simultaneously a harmonic of 2 and 4, and the mirror image of 5 in the interval defined by 4 and 7.

Figure 6b shows essentially the same structure as in Figure 6a, with two added lines. Line 7 is the harmonic of 5 and 6, and line 8 is the harmonic of 4 and 6.

Figure 6c shows that carriers can influence the spectrum even when they are too weak to be seen. Line 6, which is the upper carrier, does not appear in the spectrum. Nevertheless, its effect, which is the creation of mirror image line 4 in the interval defined by 1 and 6, is readily apparent. Lines 2 and 5 are harmonics of 3 and 4.

Figure 6d shows the single carrier spectrum. Due to the weakness of the PLR lines, three-line effects are not seen, a series of harmonics and half harmonics making up the spectrum, instead. Line 1 is a harmonic of 4 and 8. Line 2

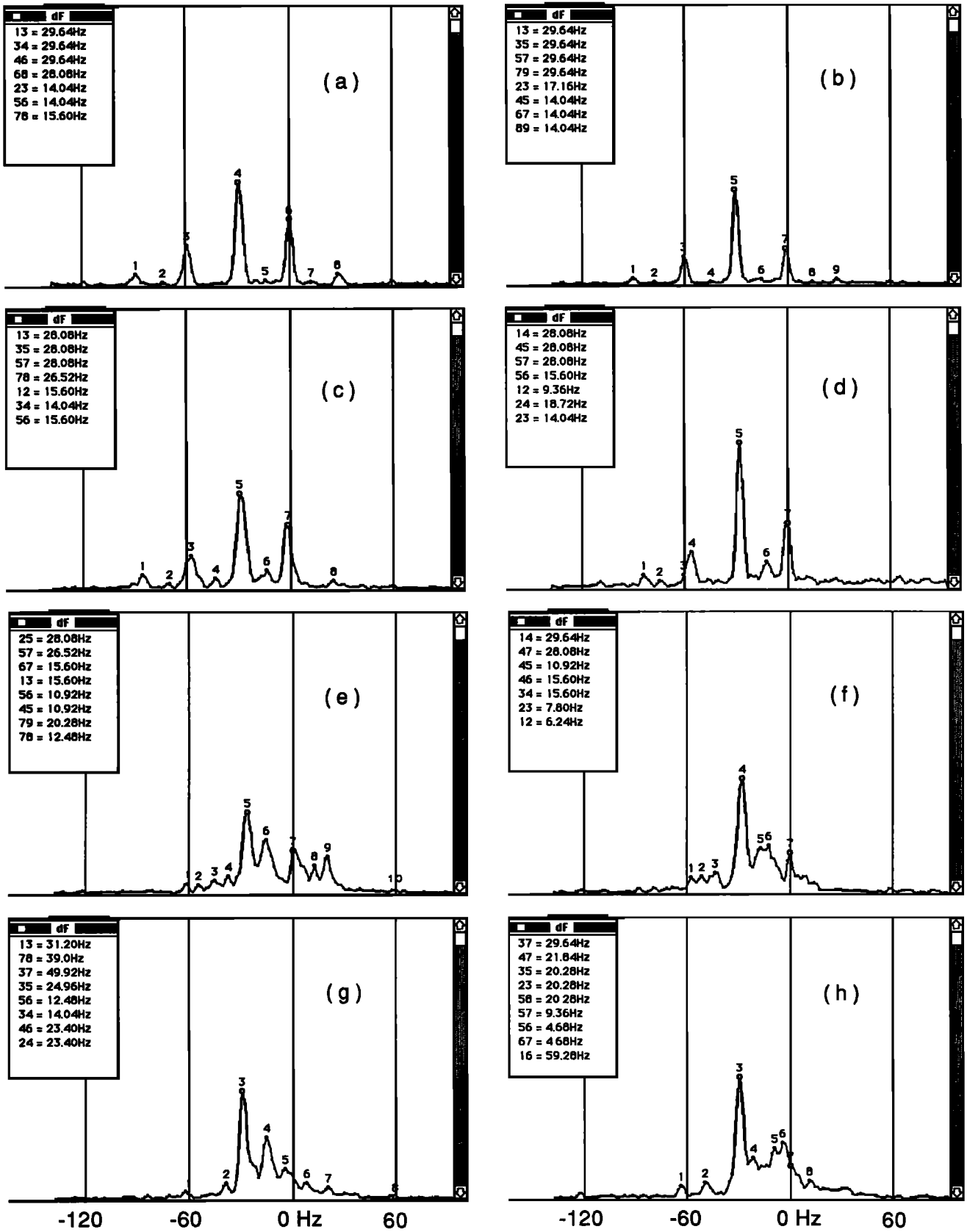


Fig. 4. Average spectra obtained from pulses shown in Figure 3: (a) and (b) 20 dB ratio, (c) and (d) 30 dB ratio, (e) and (f) 40 dB ratio, and (g) and (h) single carrier pulse. The first picture represents the first average; the second picture, the second average over each pulse. The vertical scale is linear and arbitrary. 0 Hz in those pictures corresponds to 2220 Hz absolute frequency. The carriers are denoted by small circles at the maxima. The windows in each picture contain a table of frequency differences: at the left of each equal sign are two digits representing two spectral lines; at the right is their frequency difference.

LM 08 JAN 87

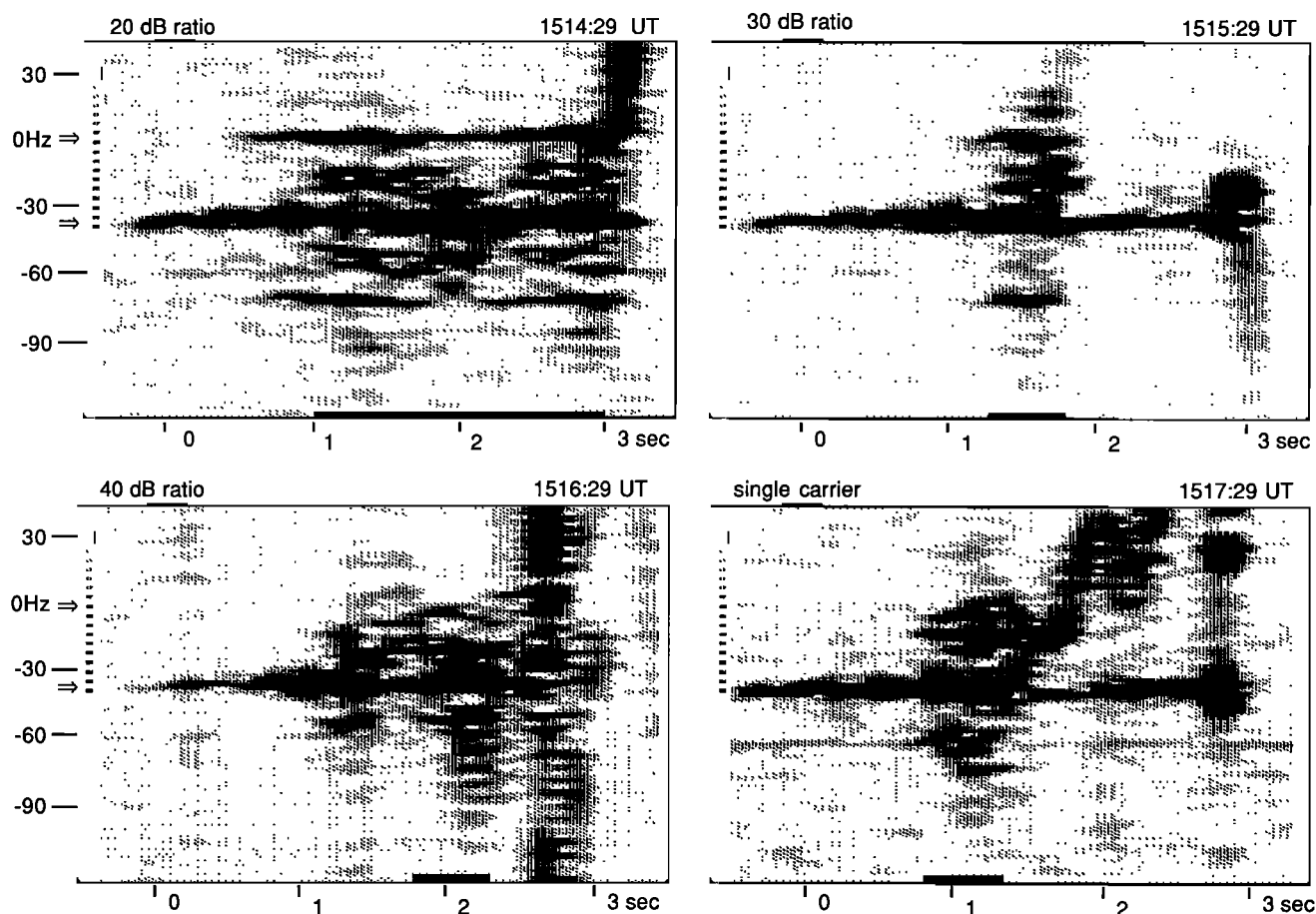


Fig. 5. Sequence of 3-s pulses with carrier separation equal to 37 Hz. 0 Hz in those pictures corresponds to 2460 Hz. The arrows point to the location of the two carriers. The horizontal bars at the bottom of each picture indicate the time intervals over which the average spectra shown in Figure 6 were taken. In all spectra the filter bandwidth was 1.56 Hz.

is a half harmonic of 1 and 3. Line 6 is a harmonic of 3 and 4. Line 7 is a half harmonic of 6 and 8. It is far-fetched to think of line 5 as the mirror image of 4, since its position is almost 5 Hz off from what would be required for that interpretation. Line 5 is almost exactly halfway between lines 4 and 8, and should therefore be thought of as a half harmonic of those two lines.

5. SUMMARY

The sideband spectra described above can be summarized as follows:

1. Sideband spectra are a consequence of the interaction of two or more lines. No real single-frequency sidebands have yet been identified.
2. Lines which are not readily seen in the measured spectra (30 dB or more below the stronger lines) can have an appreciable effect in sideband formation.
3. PLR is involved in virtually all sideband spectra. Its presence is fundamental in the creation of "single carrier" sidebands.
4. If several lines with frequencies Ω_i , $i = 1 \dots n$, measured from one of the carriers, interact creating a new line, its frequency Ω will be given by equation (1):

$$m\Omega = m_1\Omega_1 + \dots + m_n\Omega_n$$

where m and m_i are arbitrary integers ($m \neq 0$).

5. New line amplitudes depend on the combined effects of parent line intensities, frequency separations, and the electron distribution. The instability of the latter is thought to be the main cause for the imperfect reproducibility of the sideband spectra observed and described in this paper.

6. CONCLUDING REMARKS

In this paper, spectral data were presented together with an equation from which the observed frequencies in the spectra can be derived. The striking results are that vanishingly small lines can contribute to spectra formation, with no such thing as a single-frequency sideband spectrum being ever found in the data. This may explain why theories for single-frequency sidebands have not met with success when applied to sidebands observed in ducted radiation received from Siple Station.

Theories, such as the ones put forward by Nunn [1974], Brinca [1972], Das [1968], etc., describe sidebands as coming from interactions between a single carrier and the underly-

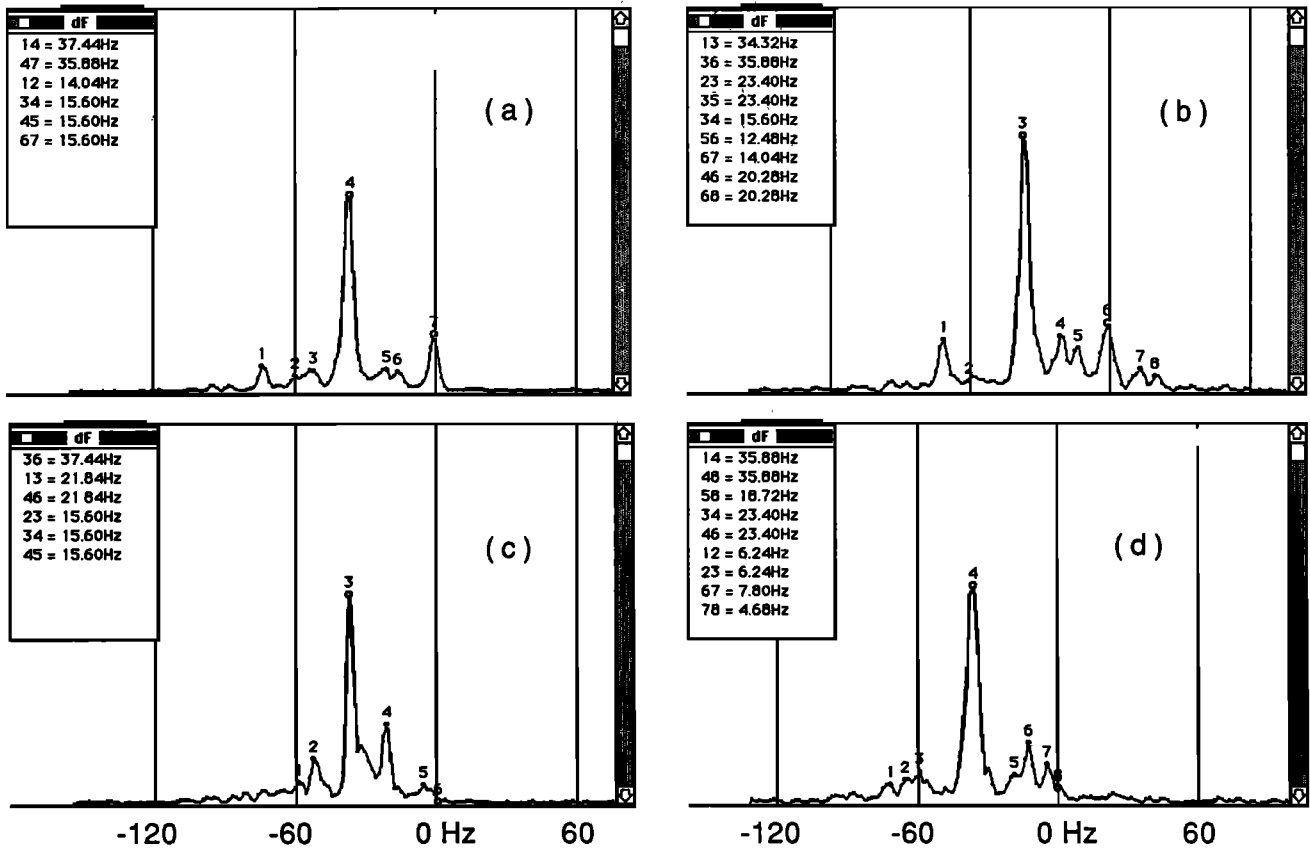


Fig. 6. Average spectra obtained from pulses shown in Figure 5: (a) 20 dB ratio, (b) 30 dB ratio, (c) 40dB ratio, and (d) single carrier pulse. The vertical scale is linear and arbitrary. 0 Hz in those pictures corresponds to 2460 Hz absolute frequency. The carriers are denoted by small circles at the maxima. The windows in each picture contain a table of frequency differences: at the left of each equal sign are two digits representing two spectral lines; at the right is their frequency difference.

ing continuous electron distribution present in the magnetosphere. Their predictions do not match the data in two main respects: First, the resulting expressions for the sideband-carrier frequency separation depend on v_{\perp} , the projection of the electron velocity in the direction perpendicular to the magnetic field of the Earth. This velocity has a continuous distribution, and after integration, should create a hump next to the carrier, instead of a sideband. This does not agree with the observed data, which show very well defined lines with widths comparable to the carrier line width. Second, such theories have as their only frequency parameter the trapping frequency of the carrier, dependent on its amplitude. This implies that any calculable frequency in those theories will be a function of the carrier amplitude, making impossible the description of sidebands that do not shift when the carrier oscillates in amplitude as seen in the data in this paper or others such as Park [1981].

The approach presented in this paper, describing sidebands as coming from a line-line interaction, does not suffer from any of the mentioned drawbacks and is in good agreement with the data. A forthcoming paper will describe its theoretical roots and implications in a systematic and general manner.

Acknowledgments. The authors thank their StarLab colleagues for helpful discussions, W. Burgess for providing access to his data acquisition system, and G. Walker for help in preparing the

manuscript. The work was sponsored by the Division of Polar Programs of the National Science Foundation under grant DPP-86-13783.

The Editor thanks G. Morales and P. K. Shukla for their assistance in evaluating this paper.

REFERENCES

- Berry, M. V., Regular and irregular motion, in *Topics in Non-linear Dynamics*, edited by S. Jorna, pp. 16-120, American Institute of Physics, New York, 1978.
- Brinca, A. L., Whistler side-band growth due to nonlinear wave-particle interaction, *J. Geophys. Res.*, **77**, 3508, 1972.
- Chirikov, B. V., A universal instability of many-dimensional oscillator systems, *Phys. Rep.*, **52**, 263, 1979.
- Das, A. C., A mechanism for VLF emissions, *J. Geophys. Res.*, **73**, 7457, 1968.
- Helliwell, R. A., U. S. Inan, J. P. Katsufakis, and D. L. Carpenter, Beat excitation of whistler mode sidebands using the Siple VLF transmitter, *J. Geophys. Res.*, **91**, 143, 1986.
- Nunn, D., A self-consistent theory of triggered VLF emissions, *Planet. Space Sci.*, **22**, 349, 1974.
- Park, C. G., Generation of whistler mode sidebands in the magnetosphere, *J. Geophys. Res.*, **86**, 2286, 1981.

R. A. Helliwell and L. A. D. Sá, STAR Laboratory, Stanford University, Stanford, CA 94305.

(Received October 9, 1987;
revised December 21, 1987;
accepted December 21, 1987.)